Optimized Lithium(I) Recovery from Geothermal Brine of Germencik, Türkiye, Utilizing an Aminomethyl phosphonic Acid Chelating Resin

Yaşar Kemal Recepoğlu

Published online: 16 Sep 2024.

Submit your article to this journal ⬚

Article views: 220

View related articles ⬚

View Crossmark data ⬚

Taylor & Francis
Taylor & Francis Group

Check for updates

Optimized Lithium(I) Recovery from Geothermal Brine of Germencik, Türkiye, Utilizing an Aminomethyl phosphonic Acid Chelating Resin

Yaşar Kemal Recepoğlu (ID)

Faculty of Engineering, Department of Chemical Engineering, Izmir Institute of Technology, Izmir, Türkiye

ABSTRACT

This study investigates the performance of Lewatit TP 260 ion exchange resin for the efficient recovery of lithium (Li(I)) from geothermal water sourced from the Germencik Geothermal Power Plant in Türkiye. A series of batch sorption experiments were performed to evaluate the influence of key parameters, including resin dosage, solution pH, temperature, initial Li(I) concentration, and contact time, on the Li(I) recovery process. The optimal conditions were determined to be a resin dose of 0.5 g per 25 mL of geothermal water, pH in the range of 6–8, and a temperature of 25°C. Under these conditions, the resin achieved a maximum Li(I) recovery rate of 71% from the geothermal water. Sorption isotherms were further analyzed using the Langmuir, Freundlich, and Dubinin-Radushkevich (D-R) models. Among these, the Langmuir model provided the best fit (R^2 = 0.9841), suggesting a maximum sorption capacity (q_m) of 4.31 mg/g. Continuous recovery experiments conducted in column mode confirmed the practical applicability of Lewatit TP 260, achieving a total sorption capacity of 0.41 mg Li(I)/mL resin. The findings exhibit the potential of this resin as a viable sorbent for sustainable Li(I) extraction from geothermal brines, supporting the development of green energy technologies and contributing to the circular economy.

Introduction

Lithium(I) (Li(I)) is a critical element that has garnered significant attention due to its vital role in modern technology and energy storage solutions.[1] As a lightweight and highly reactive metal, Li(I) is integral to the production of Li(I)-ion batteries, which power a wide range of electronic devices, including smartphones, laptops, and electric vehicles. They are favored for their high energy density, long cycle life, and lightweight properties. These batteries are essential for portable electronics, grid storage solutions, and electric vehicles, driving the green energy revolution.[2–5] Beyond batteries, Li(I) is used in the manufacture of glass and ceramics, where it improves the thermal and

mechanical properties of the final products.[6,7] Furthermore, Li(I) compounds are employed in the pharmaceutical industry for treating mental disorders and in the aerospace industry for high-performance materials.[8,9] The demand for Li(I) is projected to increase exponentially as the world transitions towards renewable energy sources and electric mobility, highlighting the need for efficient and sustainable Li(I) extraction methods.[10–12]

Li(I) can be extracted from two primary sources: Li(I)-bearing rocks (hard rock mining) and Li(I)-rich brines (hydrometallurgy).[13] The primary sources of Li(I) in hard rock mining are spodumene, petalite, and lepidolite.[14] The extraction process involves conventional mining techniques followed by crushing, grinding, and beneficiation to produce a Li(I) concentrate. This concentrate is then subjected to a series of chemical processes to extract Li(I) compounds, including roasting and leaching. However, hard rock mining is energy-intensive and can have significant environmental impacts, including habitat destruction and high carbon emissions.[15–18] On the other hand, Li(I)-rich brines are typically found in salt flats (salars) in arid regions, such as those in the Li(I) Triangle (Argentina, Bolivia, and Chile).[19] The extraction from brines involves pumping the Li(I)-rich brine to the surface and concentrating it through solar evaporation. The concentrated brine is then processed to precipitate lithium carbonate (Li_2CO_3) or lithium hydroxide (LiOH).[20] Brine extraction is less energy-intensive than hard rock mining but has its own environmental concerns, including water usage and potential impacts on local ecosystems and water tables.[21]

In recent years, geothermal water has emerged as a promising and sustainable source of Li(I). Geothermal waters, often considered waste from geothermal power plants, can contain significant Li(I) concentrations.[22,23] The extraction of Li(I) from geothermal water offers several benefits regarding sustainability as it utilizes an existing resource, minimizing environmental disruption and reducing the carbon footprint associated with Li(I) extraction and synergy with renewable energy as it can be integrated with geothermal energy production, providing a dual benefit of renewable energy and Li(I) recovery.

One of the innovative methods for extracting Li(I) from brines, such as geothermal water and seawater, is the use of ion exchange resins. Diaion HP2MG resin was impregnated with 1-phenyl-1,3-tetradecanedione (C11phβDK) and tri-n-octylphosphine oxide (TOPO) for the selective adsorption of Li(I) in aqueous chloride media. The resin absorbed 4.58 mg/g of each extractant, with maximum Li(I) adsorption of 4.17 mg/g, nearly matching the extractant content.[24] In later studies, a column packed with a synergistic solvent-impregnated resin (SIR) C11phβDK and TOPO were also used for the selective recovery of Li(I) from spent Li(I)-ion batteries.[25] So far, commercial ion exchange resins Lewatit K2629, TP 207, and TP 208 have been utilized to recover Li(I) from real brines. The sorption yield of Li(I) ranges from 30% to 55% and from 52% to 80%,

depending on the type and amount of resin used. TP 208 demonstrated the highest Li(I) sorption efficiency and loading capacity, while K2629 showed the lowest sorption efficiency and loading capacity.[26] Ion exchange resins exhibit varying selectivity coefficients based on their cation-exchange groups. The primary factors influencing ionic selectivity are the nature of the acidic functional group and the structural density, which is largely dictated by the degree of cross-linking. For resins with strongly acidic groups, such as sulfonic acid, the affinity for alkali ions typically follows the order K >> Na > Li. In contrast, resins with carboxylic, phosphonous, or phosphonic acid groups display an opposite selectivity trend, particularly favoring Li(I) ions. The ability of Lewatit TP 260, an aminomethyl phosphonic acid-containing chelating resin, to remove Li(I) from a simulated Li(I) bearing solution was reported in the literature.[27]

This research article aims to explore the potential of Lewatit TP 260 ion exchange resin in recovering Li(I) from the geothermal water of Germencik, Türkiye, for the first time as a practical application. Despite the classical nature of the experiment, applying the commercial resin to actual geothermal brine yields novel and significant findings that offer valuable engineering insights, suggesting potential advancements in the practical use of this resin in geothermal brine systems. The principles of ion exchange technology and the performance of the resin were investigated by assessing the batch mode process parameters of resin dose, temperature, initial Li(I) concentration, pH, and contact time, along with desorption and regeneration studies. To develop a sustainable and efficient method for harnessing a critical resource in the era of renewable energy and technological advancement, a column mode operation was also conducted using the resin for Li(I) recovery from geothermal water.

Experimental

Materials

Hydrochloric acid (HCl, 37%), lithium chloride (LiCl, 99%), sodium chloride (NaCl, 99%), sodium hydroxide (NaOH, 99%), and sulfuric acid (H$_2$SO$_4$, 95–97%) were supplied from Merck. Li(I) selective Lewatit MonoPlus TP 260 ion exchange resin was provided by LANXESS GmbH Production, Technology, Safety & Environment, Germany. The characteristics of the resin based on the catalog are given in Table 1.

Geothermal water obtained from the Germencik geothermal power plant, Türkiye, was used in the experimental studies whose physicochemical properties at room temperature are given in Table 2. The temperature of the geothermal fluid is around 90°C in the well; however, after sampling from its source, the water was left to cool down to room temperature naturally and brought to the laboratory for lab-scale experiments.

Table 1. The physicochemical properties of Lewatit TP 260 ion exchange resin.

Matrix	Cross-linked polystyrene
Functional group	Aminomethylphosphonic acid
Ionic form	Na^+
Total capacity	2.3 eq/L (H^+-form)
Water retention	59 – 61%
Bulk density	720 g/L
Bead size	0.4 – 1.25 mm
Effective size	0.55 ± 0.05 mm
pH range	0 – 14
Storability	−20°C − 40°C
Operating temperature	max. 80°C

Table 2. Physicochemical properties of the geothermal water sample taken from Germencik geothermal power plant, Türkiye, at room temperature.

Cation species	Concentration (mg/L)	Anion species	Concentration (mg/L)
[a]Li^+	**6.20**	[b]HCO_3^-	1264.10
[a]Na^+	980.26	[a]Cl^-	1254.99
[a]K^+	67.63	[a]F^-	9.37
[a]Ca^{2+}	20.34	[a]NO_3^-	***N.D.**
[a]Mg^{2+}	2.70	[a]SO_4^{2-}	36.43
[a]NH_4^+	***N.D.**	[a]PO_4^{3-}	***N.D.**
[c]pH		8.94	
[d]EC (mS/cm)		2.79	
[d]Salinity (ppt)		1.5	
[b]Total alkalinity (mg/L as $CaCO_3$)		1036.15	
[e]B (mg/L)		39.48	
[e]As (μg/L)		110	
[f]SiO_2 (mg/L)		152	

[a]Ion Chromatography (Thermo Scientific Dionex ICS-5000), [b]Titrimetric method, [c]pH meter (Thermo, Orion Star A111), [d]Multimeter (YSI Model 30M), [e]ICP-OES (Agilent Technologies, 5110), [f]Spectrophotometer (Hach-DR5000), *****not determined.

Methods

Batch mode sorption/desorption studies

Batch sorption experiments were conducted to evaluate the efficiency of Lewatit TP 260 ion exchange resin for Li(I) recovery from geothermal water. The experiments were designed to assess the impact of various parameters, including resin dose, pH, temperature, initial Li(I) concentration, and contact time. Different doses of dry Lewatit TP 260 resin (0.05 g, 0.1 g, 0.25 g, 0.5 g, and 0.75 g) were added to 50 mL plastic bottles containing 25 mL of geothermal water, and the bottles were shaken in a water bath at 180 rpm for 24 h. The effect of pH on Li(I) sorption was studied by adjusting the pH of the geothermal water to 2, 4, 6, 8, 10, and 12 using 0.1 M HCl or 0.1 M NaOH solutions, with experiments conducted at the optimized dry resin dose at 25°C for 24 h. Moreover, experiments were done at 25°C, 35°C, and 45°C to study the effect of temperature using a temperature-controlled water bath. The influence of initial Li(I) concentration was examined by preparing geothermal water samples with Li(I) concentrations ranging from 20 mg/L to 100 mg/L and

conducting sorption experiments at the optimized dry resin dose with different temperatures for 24 h. The impact of contact time (sorption kinetic) was investigated using geothermal water spiked with LiCl containing 100 mg/L Li(I) initially by allowing the sorption process at 20 g/L dry resin dose to proceed for 1440 min with samples withdrawn at 0, 3, 6, 9, 12, 15, 20, 30, 45, 60, 90, 120, 180, 240, 360, 480, 1440 min time intervals to measure residual Li(I) concentration. For each experiment, after the specified contact time, the resin was separated from the solution by filtration, and the Li(I) concentration in the filtrate was determined using Inductively Coupled Plasma Optical Emission Spectroscopy (ICP-OES). The recovery percentage and the amount of Li(I) adsorbed by the resin were calculated based on the difference between the initial and final Li(I) concentrations in the solution, as given in the following equations:

$$R(\%) = \frac{C_0 - C_e}{C_o} \times 100 \tag{1}$$

$$q_e = \frac{(C_0 - C_e)V}{m} \tag{2}$$

where $R(\%)$ is the recovery percentage of Li(I) from geothermal water. C_0 and C_e are the initial and final equilibrium Li(I) concentrations (mg/L) in the solution, respectively. q_e is the amount of Li(I) adsorbed by the resin at equilibrium (mg/g), V is the solution volume (L), and m is the dry resin amount (g).

Regeneration of Lewatit TP 260 and desorption of Li(I) studies were conducted using various desorption solutions. The exhausted resin obtained from the kinetic test was washed with deionized water, dried at 40°C overnight, and then subjected to desorption using 0.05 M, 0.1 M, and 0.5 M HCl, H_2SO_4, and NaCl. Each desorption process involved agitating the resin (0.5 g) in the desorption solution (25 mL) for 24 h at 25°C, followed by filtration and measurement of Li(I) concentration in the desorption solution using ICP-OES. The desorption efficiency was calculated as the percentage of Li(I) removed from the resin.

Column mode sorption/desorption studies

Column mode experiments were conducted to evaluate the continuous sorption and desorption of Li(I) from geothermal water using Lewatit TP 260 ion exchange resin. A glass column with an inner diameter of 0.7 cm and a height of 12 cm was packed with previously wetted Lewatit TP 260 resin, maintaining a bed height of 1.5 cm (wet volume: 0.58 cm^3). For the sorption studies, geothermal water with an influent Li(I) concentration of 6.2 mg/L was passed through the resin column downward at a flow rate of 0.25 mL/min (SV: 25.8

BV/h) using a peristaltic pump (SHENCHEN). Three milliliters of effluent samples were collected regularly with the help of a fraction collector (BÜCHI C-660) and analyzed for Li(I) concentration using a flame photometer (JENWAY PFP7). The breakthrough point, defined as the time when the effluent Li(I) concentration reached 40% of the influent concentration, was determined from the breakthrough curve, and the sorption capacity of the resin was calculated based on the treated water volume and effluent Li(I) concentration.

The bed volume (BV, mL of geothermal brine per mL of resin) was determined using Eq. (3)[28]:

$$BV = \frac{Qt}{V} \qquad (3)$$

where Q represents the feed solution flow rate (mL/min), t is the operating time (min), and V is the wet volume of the resin (mL). In addition, the space velocity (SV, min^{-1}, or h^{-1}) is calculated as the ratio of the feed solution flow rate to the wet volume of the resin, as shown in Eq. (4).[28]

$$SV = \frac{Q}{V} \qquad (4)$$

After the sorption process, the packed column was thoroughly washed with deionized water. Then, desorption studies were conducted by passing 5% H_2SO_4 through the resin column at a flow rate of 0.12 mL/min until the Li(I) concentration in the effluent approached zero. The total volume of desorption solution used and the Li(I) concentration in the desorption effluent were recorded, and the desorption efficiency was calculated as the percentage of Li(I) recovered from the resin.

Results and discussion

The effect of resin dose

The effect of varying Lewatit TP 260 ion exchange resin doses on Li (I) recovery from geothermal water was investigated. The percentage of Li(I) recovery at each resin dose is presented in Figure 1. As shown in the figure, Li(I) recovery increased with the resin dose. At a dose of 0.05 g in 25 mL geothermal water, the Li(I) recovery was approximately 22%. Increasing the resin dose to 0.1 g resulted in a recovery rate of about 35%. Further increments in the resin dose to 0.25 g and 0.5 g yielded approximately 52% and 71% Li(I) recovery rates, respectively. The highest dose tested, 0.75 g, achieved a Li(I) recovery rate of around 79.5%. Notably, the recovery rate experienced a sharp increase at lower doses, particularly between 0 and 0.25 g, attributed to the abundance of available active sites on the resin. However, beyond 0.5 g, the
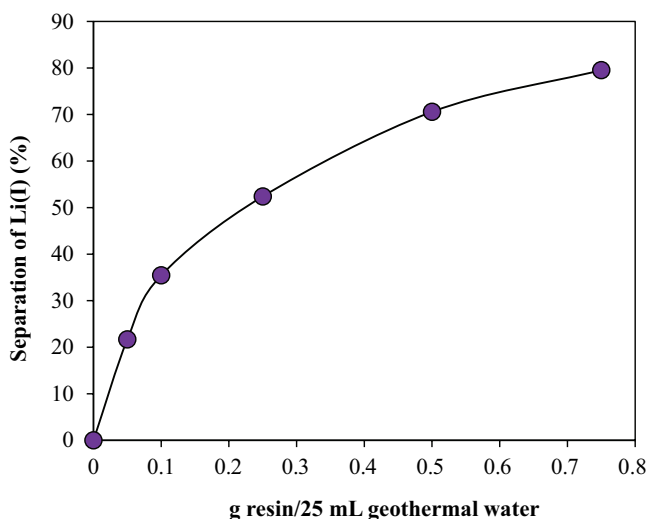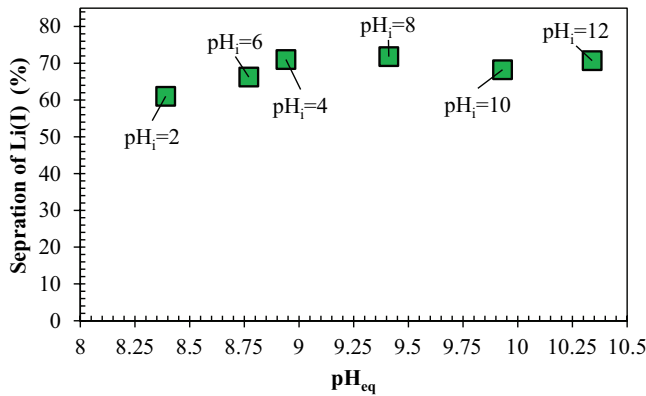
Figure 1. Effect of Lewatit TP 260 ion exchange resin dose on the separation of Li(I) from geothermal water.

increment in recovery rate began to taper off, indicating the approaching saturation of the resin's active sites. Based on the balance between recovery efficiency and practical application, the optimum resin dose was identified as 0.5 g per 25 mL of geothermal water, achieving a substantial recovery rate of approximately 71%. These findings align with theoretical expectations and previous studies, highlighting the critical role of active site availability in ion exchange processes.[27,29,30] The practical implications suggest that while increasing resin dose enhances recovery, there is a point of diminishing returns, making it essential to balance resin cost with desired recovery efficiency.

The effect of pH

The impact of pH on Li (I) recovery from geothermal water using Lewatit TP 260 ion exchange resin, which contains an aminomethylphosphonic acid functional group, was evaluated, revealing that Li(I) recovery efficiency remained relatively stable across the pH range of 4 to 12. Figure 2 shows that recovery rates were approximately 71% at pH 4, 66% at pH 6, 72% at pH 8, 68% at pH 10, and 71% at pH 12, indicating consistent resin performance regardless of pH fluctuations. The stability of Li(I) recovery across this pH range can be attributed to the aminomethylphosphonic acid functional group's ability to maintain its ion exchange capacity effectively despite the protonation and deprotonation that occur at different pH levels. This resilience suggests that the functional group's structure provides sufficient buffering to handle pH variations without significant loss of binding efficiency,

Figure 2. Effect of pH on Li(I) recovery from geothermal water using Lewatit TP 260 ion exchange resin.

which is advantageous for practical applications by reducing the need for stringent pH control. The results imply that the resin can be efficiently utilized in diverse geothermal water conditions, simplifying the process and potentially lowering operational costs. Although the optimal pH conditions for maximum Li(I) recovery were identified at pH 8, achieving about 72% recovery, a relatively wide pH range supports the resin's suitability for broad applications.

The effect of temperature and initial concentration

The effect of temperature on Li(I) recovery from geothermal water using Lewatit TP 260 ion exchange resin was evaluated alongside the different initial Li(I) concentrations. Sorption isotherms (q_e vs. C_e) at different temperatures were plotted in Figure 3(a). The sorption capacity (q_e) of the resin was determined at three different temperatures: 25°C, 35°C, and 45°C, across a range of equilibrium Li(I) concentrations (C_e). The results indicate that increasing temperature decreases Li(I) sorption capacity. The resin exhibited higher sorption capacities at lower temperatures than at higher temperatures across the entire concentration range. Specifically, the maximum sorption capacity reached approximately 3.58 mg Li(I)/g resin at 25°C, 3.47 mg Li/g resin at 35°C, and 3.23 mg Li(I)/g resin at 45°C for the highest tested equilibrium concentration. This adverse effect of temperature on Li(I) recovery can be attributed to the exothermic nature of the ion exchange process, where higher temperatures reduce the resin's affinity for Li(I) ions. The trend suggests that lower temperatures favor Li(I) binding to the resin's amino-methylphosphonic acid functional groups, enhancing recovery efficiency. The increased sorption capacity with higher initial Li(I) concentrations indicates that the resin's binding sites are progressively utilized with increasing Li(I)
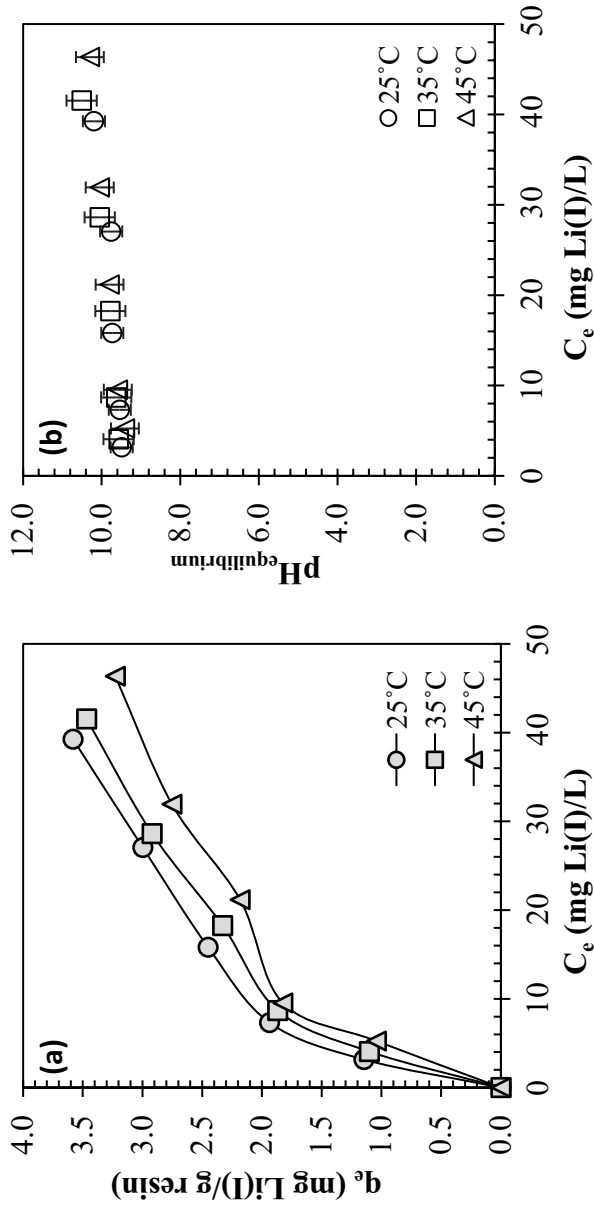
Figure 3. (a) Sorption isotherms of Lewatit TP 260 resin for Li(I) recovery from geothermal water at different temperatures, (b) equilibrium pH vs. equilibrium concentration (C_e) at different temperatures.

availability. This combined effect of temperature and initial concentration on Li(I) recovery provides valuable insights for optimizing geothermal water treatment processes using Lewatit TP 260 resin, highlighting the importance of maintaining lower operational temperatures to maximize Li(I) recovery. On the other hand, Figure 3(b) shows that the sorption isotherms obtained at different temperatures had almost the same equilibrium pH values between 9.7 and 9.9 on average, which validates the sorption isotherms for the cation exchange resin. As the resin was originally in the form of Na^+, there was no considerable pH change at equilibrium when Na^+ ions were exchanged with Li(I) ions in the geothermal water, which shows neutral behavior in the medium.

Sorption isotherms

The sorption isotherms of Lewatit TP 260 ion exchange resin for Li(I) ions were mathematically represented by the Langmuir, Freundlich, and Dubinin-Radushkevich (D-R) models. The experimental data align well with the Langmuir (Eq. (5)),[31] Freundlich (Eq. (6)),[32] and D-R (Eqs. (7–9))[33] isotherm models.

$$\frac{1}{q_e} = \left(\frac{1}{K_L q_m}\right)\frac{1}{C_e} + \frac{1}{q_m} \tag{5}$$

$$ln q_e = ln K_F + \frac{1}{n}(ln C_e) \tag{6}$$

$$ln q_e = ln q_s - k_{ads}\varepsilon^2 \tag{7}$$

$$\varepsilon = RTln\left(1 + \frac{1}{C_e}\right) \tag{8}$$

$$E = \frac{1}{\sqrt{2k_{ads}}} \tag{9}$$

where q_m is the maximum sorption capacity attributing to the maximum monolayer coverage (mg/g); K_L is the Langmuir constant (L/mg). K_F ((mg/g) $(L/mg)^{1/n}$) and n are the Freundlich constants related to sorption capacity and intensity, respectively. q_s is the theoretical isotherm saturation capacity (mg/g), k_{ads} is the D-R isotherm constant (mol²/kJ²), E is the apparent energy of the sorption (kJ/mol), R is the universal gas constant (8.314 kJ/kmol.K), and T is the absolute temperature (K). With these, isotherms parameters useful for Li(I) sorption system design for Lewatit TP 260 ion exchange resin were obtained and reported in Table 3.

Table 3. Isotherms models with associated parameters and values for sorption of Li(I) on Lewatit TP 260 ion exchange resin.

Isotherm model	25°C	35°C	45°C
Langmuir	4.31	4.43	4.19
q_{max} (mg g^{-1})	0.101	0.075	0.064
K_L (L mg^{-1})	0.9841	0.9805	0.9732
R^2			
Freundlich	0.747	0.605	0.524
K_F ((mg/g) (L/mg)$^{1/n}$)	2.325	2.119	2.086
n	0.9811	0.9795	0.9446
R^2			
D-R	0.0055	0.0062	0.0065
β (mol^2 kJ^{-2})	9.55	8.99	8.76
E (kJ mol^{-1})	8.79	9.45	9.01
q_s (mg g^{-1})	0.9885	0.9857	0.9545
R^2			

The maximum sorption capacity (q_m) and the constant related to the binding energy of the sorption system (K_L) estimated by Langmuir isotherm with a relatively higher linear regression coefficient ranging from 0.9841 to 0.9732 for Li(I), have been determined to be in the range of 4.31–4.19 mg/g and 0.101–0.064 L/mg, respectively, for the Li(I)-resin system. The other Lewatit-type ion exchange resins, such as K2629, TP 207, and TP 208, exhibited a maximum sorption capacity of 1.84, 2.54, and 1.23 mg/g, respectively.[26] The separation factor (R_L) has been derived from the Langmuir model using the following equation:

$$R_L = \frac{1}{1 + K_L C_0} \tag{10}$$

The R_L values were between 0 and 1 for the initial Li(I) concentration range of 20 to 100 ppm at all studied temperatures, indicating favorable adsorption.

Freundlich isotherm fittings resulted in the sorption of Li(I) using Lewatit TP 260 resin, with a linear regression coefficient ranging from 0.9811 to 0.9446. The Freundlich constants K_F and n are calculated to be 0.747–0.524 and 2.325–2.086, respectively. Since n lies between 1 and 10, the sorption of Li(I) on the resin is considered favorable. In addition, 1/n is a heterogeneity parameter; hence, a value smaller than 1 indicates greater heterogeneity in the sorption process.

The experimental data fitted to the D-R isotherm model allow for the determination of the nature (physical or chemical) of the sorption process on the sorbent surface and can be used to calculate the mean free energy of adsorption (E). The mechanism of adsorbate binding is inferred from the value of this parameter: if E <8 kJ/mol, the sorption process is physical; if 8 <16 kJ/mol, the process is governed by ion exchange; and if 1640 kJ/mol, chemisorption occurs.[34] Given that E values determined at different temperatures to be in the range of 8.76–9.55 kJ/mol, it is concluded that ion exchange governs the mechanism of Li(I) sorption on Lewatit TP 260 resin.

The q_s value (8.79–9.01 mg/g) indicates the porosity of the resin; a larger q_s value signifies more developed active binding sites. Above all, the Langmuir isotherm fitted the experimental data better than the Freundlich and D-R isotherms that describe Type-I sorption behavior for Li(I) and Lewatit TP 260 resin.

Sorption thermodynamics

The investigation explored the sorption behavior of Li(I) ions across a temperature range of 25°C to 45°C using Lewatit TP 260 resin. The maximum sorption capacities obtained from Langmuir revealed a decrease in sorption capacity from 4.31 to 4.19 mg/g as the solution temperature rose, indicating an exothermic sorption process of Li(I) ions onto the resin. This decrease in sorption rate with temperature can be attributed to the weakening of attractive forces between the active sites of the resin and the Li(I) ions and between the neighboring molecules of the adsorbed phases.

The variation in sorption levels with temperature has been explained through the analysis of thermodynamic parameters: the change in enthalpy ($\Delta H°$, kJ/mol), entropy ($\Delta S°$, kJ/mol.K), and Gibbs free energy ($\Delta G°$, kJ/mol.K). These parameters were calculated using the following equations.

$$\Delta G° = \Delta H° - T\Delta S° \tag{11}$$

$$\Delta G° = -RTlnK_D \tag{12}$$

$$lnK_D = \frac{\Delta S°}{R} - \frac{\Delta H°}{RT} \tag{13}$$

$$K_D = \frac{(1000K_L MW_{adsorbate})[Adsorbate]^0}{\gamma} \tag{14}$$

Where K_D is the equilibrium constant (dimensionless), γ is the coefficient of activity (dimensionless), $[Adsorbate]^0$ is the standard concentration of the adsorbate (1 mol L^{-1}). $MW_{adsorbate}$ is the molecular weight of the adsorbate (g mol^{-1}). 1000 stands for converting L mg^{-1} into L g^{-1}.

The negative $\Delta G°$values (from −16.19 to −16.07 kJ/mol) confirm the feasibility of the sorption process at various temperatures and indicate its spontaneous nature, with an increasing preference for Li(I) onto resin as the temperature rises from 25°C to 45°C. The $\Delta H°$ and $\Delta S°$ parameters were derived from the slope and intercept of the Van't Hoff plot of lnK_D versus 1/T (see Equation. 13). The negative $\Delta H°$ value −17.97 kJ/mol) across the temperature range indicates the exothermic nature of the sorption process. The relatively low absolute $\Delta H°$ value,

below 20 kJ/mol, suggests the involvement of physisorption. Therefore, the estimated $\Delta H°$ value lower than 20 kJ/mol hints at a spontaneous sorption mechanism likely involving physisorption, where chemical bonds exhibit weaker or no energies. Furthermore, the negative $\Delta S°$ value −5.97 J/mol·K) indicates a decrease in the degree of freedom of the adsorbed species, suggesting a decrease in Li(I) concentration at the solid–liquid interface and an increase in Li(I) concentration in the solid phase. This behavior is typical of physisorption and is driven by van der Waals interactions.[35]

The effect of contact time

The separation efficiency of Li(I) over time, as analyzed from the collected samples, is shown in Figure 4(a). The removal kinetics of the Lewatit TP 260 resin were remarkably fast, achieving almost 70% removal rate within 20 min. Understanding kinetic parameters is essential for predicting sorption rates and providing valuable insights for designing and modeling sorption processes. Therefore, three widely used kinetic models – the Lagergren pseudo-first-order model (Eq. (15)), the pseudo-second-order model (Eq. (16)), and the Weber and Morris intraparticle diffusion model (Eq. (17)) – were employed to analyze the experimental data related to the sorption of Li(I) onto the resin.

$$\ln(q_e - q_t) = lnq_e - k_1 t \tag{15}$$

$$\frac{t}{q_t} = \frac{1}{k_2 q_e^2} + \frac{1}{q_e} t \tag{16}$$

$$q_t = k_i t^{0.5} + C_i \tag{17}$$

where q_e (mg/g) and q_t (mg/g) are the amounts of Li(I) sorbed at equilibrium and the amount of Li(I) sorbed at time t, respectively. t is the time (min), k_1 is the constant rate of pseudo-first-order adsorption (min^{-1}), k_2 is the constant rate of the pseudo-second-order adsorption (g/(mg·min)), k_i is the intraparticle diffusion rate (mg/(g·min$^{0.5}$)), and C_i is the intercept. Figure 4(b,c) present the plots for the pseudo-first order and pseudo-second order models to examine the conformity between the experimental data and the models using linear regression. From the slope and intercept of the plot of ln(q$_e$−q$_t$) vs. t, the first-order rate constant (k$_1$) and the calculated equilibrium sorption capacities (q$_{e,cal}$) were determined. The correlation coefficient (R^2) for Li(I) sorption using the Lagergren equation was 0.9619. However, the experimental equilibrium sorption capacity (q$_{e,exp}$ = 3.32 mg/g) did not match the calculated q$_{e,cal}$ value (1.34 mg/g), suggesting that the sorption of Li(I) onto the resin

under the studied conditions did not follow first-order kinetics. Conversely, the second-order rate constant (k_2) and the $q_{e,cal}$ were determined from the linear plot of t/q_t vs. t. The kinetic sorption of Li(I) onto the resin was better described by the pseudo-second-order model, as evidenced by a higher correlation coefficient ($R^2 = 0.9995$). Moreover, the calculated sorption capacity ($q_{e,cal} = 3.53$ mg/g) based on the pseudo-second-order model was closely aligned with the experimental value ($q_{e,exp} = 3.32$ mg/g).

The primary method for discerning sorption mechanisms involves fitting experimental data into the intraparticle diffusion model (Eq. (17)) proposed by Weber and Morris in 1962.[36] Many instances in the literature have documented multi-linearity in the qt vs. $t^{0.5}$ plot. As shown in Figure 4(d), the sorption data of Li onto the resin can be delineated by two straight lines. The initial curved segment of the plot signifies external diffusion (boundary layer diffusion), while the
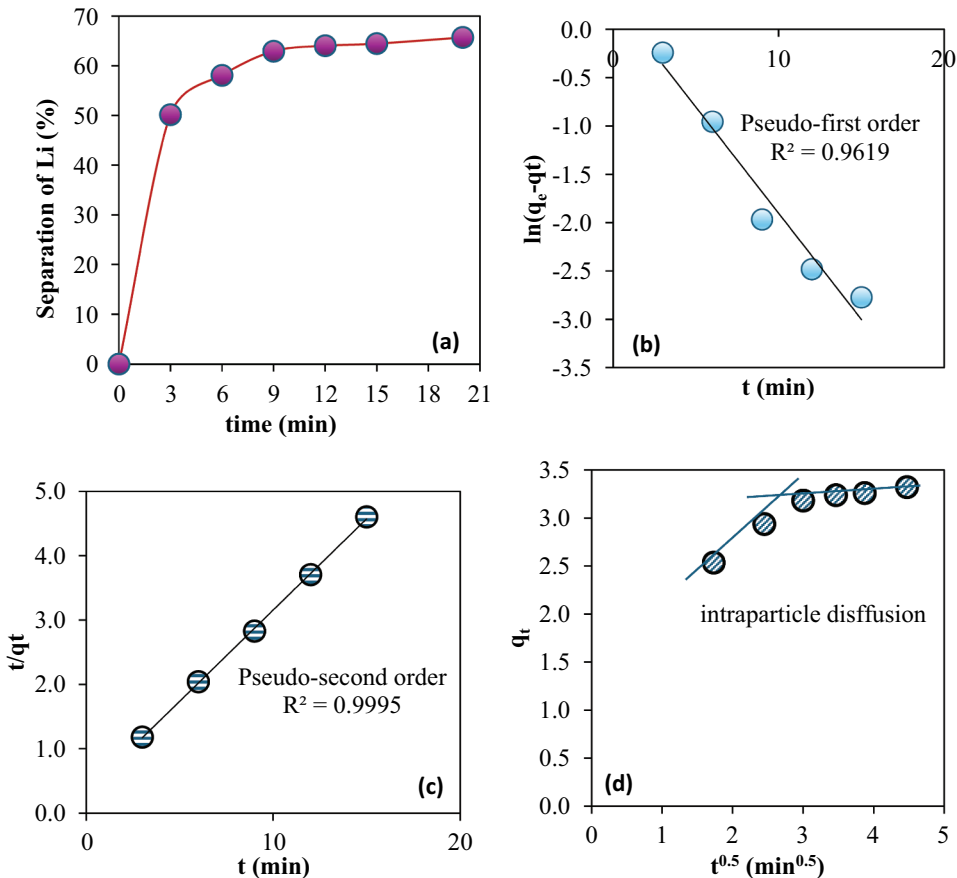
Figure 4. (a) The effect of contact time on Li(I) separation efficiency, (b) Linear plot of pseudo-first order model, (c) Linear plot of pseudo-second order model, and (d) Intraparticle diffusion kinetics of Li(I) sorption on Lewatit TP 260 resin.

Table 4. The calculated parameters and correlation coefficients of kinetic models determined for the Lewatit TP 260 resin.

Model	Parameter	Value
Pseudo-first-order	R^2	0.9619
	k_1 (min^{-1})	0.2197
	$q_{e,cal}$ (mg/g)	1.34
	$q_{e,exp}$ (mg/g)	3.32
Pseudo-second-order	R^2	0.9995
	k_2 (g/(mg·min))	0.2493
	$q_{e,cal}$ (mg/g)	3.53
	$q_{e,exp}$ (mg/g)	3.32
Intraparticle diffusion	R^2	0.9716
	k_i (mg/g min$^{0.5}$)	0.0845
	C_i (mg/g)	2.94

subsequent linear portion represents intraparticle diffusion (diffusion within the polymer network). However, the data points do not intersect the origin, indicating that intraparticle diffusion is not the sole limiting mechanism. Other factors, such as repulsion between Li(I) ions and/or between the sorbent and dye molecules due to concentration density, also contribute significantly. The intercept C_i provides insights into boundary layer thickness: a higher intercept suggests a more significant boundary layer effect. The value of C_i was found to be 2.94 mg/g. Furthermore, the intraparticle diffusion rate constant k_i, derived from the latter portion of the q_t vs. $t^{0.5}$ plot, was determined to be 0.0845 mg/g·min$^{0.5}$. Table 4 collects the parameters, correlation coefficients for pseudo-first order and pseudo-second order models, and intraparticle diffusion kinetics.

Desorption of Li(I) and regeneration of the resin

Figure 5 illustrates the desorption efficiency of Li(I) from Lewatit TP 260 ion exchange resin using various desorption solutions (NaCl, HCl, and H_2SO_4) at different molarities (0.05 M, 0.1 M, and 0.5 M). The results show that NaCl was ineffective for desorbing Li(I), with desorption efficiencies close to 1% across all tested molarities. In contrast, HCl and H_2SO_4 exhibited significantly higher efficiencies. At a concentration of 0.05 M, HCl achieved 62.5% desorption efficiency, whereas it was 99.9% for H_2SO_4. However, at higher concentrations of 0.1 M and 0.5 M, both acids demonstrated 99.9% desorption efficiency. These findings indicate that while NaCl was unsuitable for Li(I) desorption from Lewatit TP 260, both HCl and H_2SO_4 are highly effective, particularly at higher molarities, making them the preferred desorption agents for efficient Li(I) recovery and regeneration of the resin.
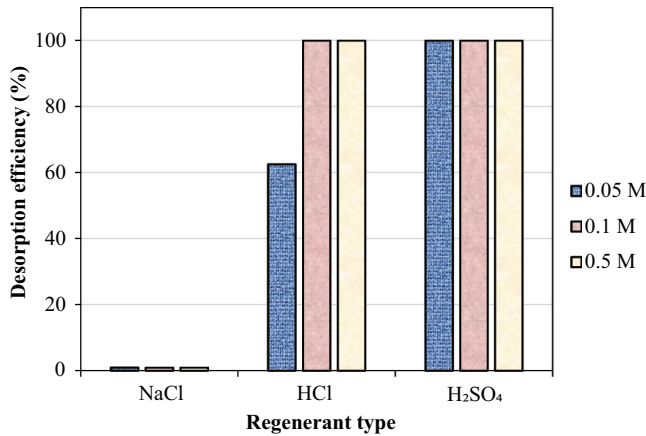
Figure 5. Li(I) desorption efficiency from Lewatit TP 260 ion exchange resin using various desorption solutions (NaCl, HCl, and H2SO4) at different molarities (0.05 M, 0.1 M, and 0.5 M).

Chromatographic separation and recovery of Li(I) from geothermal water

The chromatographic separation of Li(I) from geothermal water using Lewatit TP 260 ion exchange resin is illustrated through the breakthrough and elution curves in Figure 6(a,b), respectively. In the case of sorption, initially, C/C_0 is close to 0, indicating effective adsorption. As BV increases, C/C_0 rises gradually, reaching approximately 0.9 at 250 BV, signaling the nearing saturation of the resin. At 300 BV, C/C_0 approaches 1, marking complete saturation. At the breakthrough point, the breakthrough time is defined by the ratio of the effluent concentration to the influent concentration. Specifically,
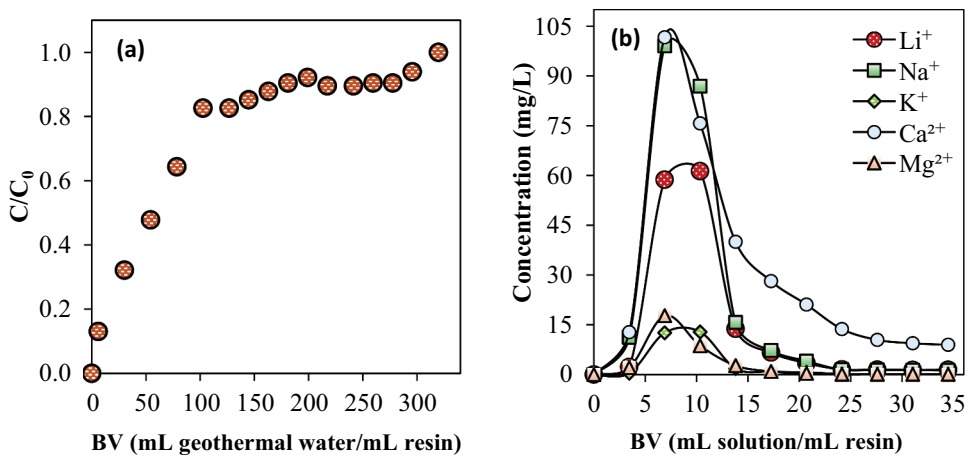
Figure 6. (a) Breakthrough curve displaying the ratio of effluent to influent Li(I) concentration (C/C0) vs bed volume (BV), (b) Elution curve depicting the concentration of Li(I) and other major cations as a function of bed volume for the chromatographic separation of Li(I) from geothermal water using Lewatit TP 260 ion exchange resin.

a breakthrough time value of 0.05 is typically used as the threshold ratio in fixed-bed operations to remove heavy metal ions from water. However, given the focus on recovering a valuable metal, this study adopted a different approach based on the literature where the breakthrough point was accepted as the time required for the Li(I) extraction rate to decrease to 0.6.[37,38] Therefore, the breakthrough capacity was 0.17 mg Li(I)/mL resin, and BV was 43. While at the saturation point, the total capacity was found to be 0.41 mg Li(I)/mL resin with 320 BV. The degree of column utilization (breakthrough capacity/total capacity) was estimated at 41.5%. The shape of the breakthrough curve for Li(I) separation using Lewatit TP 260 ion exchange resin deviates from the classic S-shape due to several influencing factors. The presence of competing ions in geothermal water and variations in flow rate and contact time contribute to this deviation. Moreover, mass transfer limitations such as film and pore diffusion slow the adsorption process, resulting in a more gradual increase in the C/C_0 ratio rather than a sharp transition typical of an S-shaped curve. These combined factors lead to a breakthrough curve that reflects the complexities of the actual adsorption process rather than the idealized S-shape. Several strategies can be employed to enhance sorption efficiency in dynamic column operations. Optimizing the packed column for Li(I) recovery using Lewatit TP 260 resin involves refining key parameters such as column configuration, flow rate, pH, and temperature, each critical for maximizing efficiency. Adjusting the height-to-diameter ratio and resin packing density enhances contact time, improving ion exchange efficiency by ensuring sufficient interaction between the resin and brine. Variable and pulsed flow regimes optimize residence time, allowing more effective Li(I) uptake, while precise pH control enhances Li(I) selectivity by favoring optimal binding conditions. Temperature management accelerates ion exchange kinetics, which is particularly beneficial in colder brines where reaction rates are slower. Efficient resin regeneration protocols are essential to sustain performance across multiple cycles, and real-time monitoring with automation ensures consistent recovery under varying operational conditions, thereby maximizing the overall process efficiency and reliability.[39]

In the elution stage, a sharp peak of around 65 mg/L is observed at 10 BV, indicating rapid and efficient Li(I) desorption. The concentration then sharply declines, dropping below 10 mg/L by 15 BV and stabilizing around 0 mg/L after 25 BV. These results demonstrate that Lewatit TP 260 resin can effectively adsorb Li(I) from geothermal water up to around 250 BV and elute it in a concentrated form, with most Li(I) recovered within the first 15 BV of the eluting solution. Given that almost 100% elution efficiency was recorded, Li(I) can be desorbed, and the resin can be regenerated easily. On the other hand, there are other major cations, such as Na^+, K^+, Ca^{2+}, and Mg^{2+}, in the product elution solution. In the realm of Li(I) extraction from geothermal brine, the concentration factor (CF) is crucial in assessing Li(I) selectivity against other

dominant cations. The CF, defined as the ratio of the concentration of each species in the sorbent phase to that in the initial solution phase ($C_{0,i}$), serves as a key metric in evaluating the performance of ion-exchange resins or adsorbents. A higher concentration factor reflects a more selective adsorption process, wherein Li(I) ions are preferentially captured over competing cations, thereby reducing the likelihood of contamination in the final product. The total concentration of each cation in the sorbent phase or elution product solution ($C_{t,i}$, mg/L) was estimated using two peak points in the elution curve. The equations used for determining the total concentration of each cation in the sorbent phase and CF are provided below.

$$C_{t,i} = \frac{C_{1,i}V_{1,i} + C_{2,i}V_{2,i}}{V_{1,i} + V_{2,i}} \tag{18}$$

$$CF = \frac{C_{t,i}}{C_{0,i}} \tag{19}$$

where $V_{1,i}$ and $V_{2,i}$ are the fraction volumes (mL) of the two peak concentrations of cation i on the elution curve.

CF for Li(I), Mg^{2+}, Ca^{2+}, K^+, and Na^+ were calculated as 9.68, 4.90, 4.36, 0.19, and 0.09, respectively. Given that Li(I) is present in much lower concentrations in the geothermal brine than these other cations when compared, the CFs of each cation showed that the selective separation was achieved for effective recovery of Li(I). Moreover, Li(I) precipitation as Li_2CO_3 from an aqueous solution typically requires a sufficient concentration of Li(I) and CO_3^{2-} ions under controlled conditions. The solubility product (K_{sp}) of Li_2CO_3 is quite low (around 8.15×10^{-4} at 25°C), meaning it is not very soluble in water. Therefore, in principle, concentrated Li(I) (ca. 60 mg/L) could be sufficient for precipitation if the CO_3^{2-} concentration is adequately high and the solution conditions are favorable.

Conclusions

The investigation of Lewatit TP 260 ion exchange resin for Li(I) recovery from geothermal water has demonstrated significant potential for efficient and sustainable extraction processes. Batch mode experiments revealed that optimal Li(I) recovery is achieved with a resin dose of 0.5 g per 25 mL of geothermal water, within a pH range of 6–8, and at a temperature of 25°C. The maximum recovery rate recorded was 71%, highlighting the resin's effectiveness under these conditions. The Langmuir isotherm model best described the sorption capacity, with a maximum capacity of 4.31 mg/g, while Çiçek et al.[27] reported a 13.65 mg/g monolayer sorption capacity with a 5 mg Li(I)/L LiCl

Table 5. A comparative analysis of the studied sorbent (Lewatit TP 260 ion exchange resin) and various other sorbents for Li(I) recovery from brines.

Sorbent	Sorption capacity (mg/g)	Equilibrium constant*	Rate constant*	Reference
UBK 10 cation exchange resin	0.06^{PSO}	N.A.	40.08^{PSO}	[40]
Amberlite IR120 Plus resin	0.336	N.A.	N.A.	[41]
Purolite C100	0.279			
Purolite C150	0.318			
Purolite C160	0.437			
Trilite SCR-B	0.336			
Lewatit K2629	1.84^{L}	0.108^{L}	0.0600^{PSO}	[26]
Lewatit TP 207	2.54^{L}	2.434^{L}	0.1249^{PSO}	
Lewatit TP 208	1.23^{L}	0.325^{L}	0.2168^{PSO}	
Li-imprinted polymer	2.10	N.A.	N.A.	[42]
Magnetic ion imprinted polymer	4.07^{L}	0.092^{L}	0.186^{PSO}	[43]
Lewatit TP 260 resin	4.31^{L}	0.101^{L}	0.2493^{PSO}	This work

*L: Langmuir; equilibrium constant, K_L (L mg^{-1}); PSO: pseudo-second order, rate constant, k_2 (g mg^{-1} min^{-1}); N.A.: not available

solution for Lewatit TP 260 ion exchange resin. Although there is a scant field for Li(I) recovery from brines using ion-exchange polymers, the sorption capacities and kinetics of the applied sorbent, which is Lewatit TP 260, and several others recently utilized, mostly featuring commercially available ion exchange resins, are presented in Table 5. Column mode studies further validated the practical applicability of Lewatit TP 260 resin in continuous Li(I) recovery operations, with a defined breakthrough point and efficient desorption using 5% H_2SO_4. These findings support the feasibility of using Lewatit TP 260 for Li(I) extraction from geothermal brines, offering a promising approach to meeting the growing demand for Li(I) in the context of renewable energy and electric mobility advancements.

Future work should explore the long-term operational stability and economic viability of this method to further solidify its role in sustainable Li(I) recovery technologies. Investigations into the regeneration and reuse of the resin and the optimization of process parameters for large-scale applications will be crucial. In addition, the environmental impact of the entire process, from extraction to resin disposal, needs to be thoroughly assessed to ensure its sustainability.

Disclosure statement

No potential conflict of interest was reported by the author(s).

ORCID

Yaşar Kemal Recepoğlu   http://orcid.org/0000-0001-6646-0358

References

[1] Zhang, X.-Q.; Zhao, C.-Z.; Huang, J.-Q.; Zhang, Q. Recent Advances in Energy Chemical Engineering of Next-Generation Lithium Batteries. *Engineering* 2018, *4*(6), 831–847. DOI: 10.1016/j.eng.2018.10.008.

[2] Afroze, S.; Reza, M. S.; Kuterbekov, K.; Kabyshev, A.; Kubenova, M. M.; Bekmyrza, K. Z.; Azad, A. K. Emerging and Recycling of Li-Ion Batteries to Aid in Energy Storage, a Review. *Recycling* 2023, *8*(3), 48. DOI: 10.3390/recycling8030048.

[3] Liang, Y.; Zhao, C.; Yuan, H.; Chen, Y.; Zhang, W.; Huang, J.; Yu, D.; Liu, Y.; Titirici, M.; Chueh, Y. A Review of Rechargeable Batteries for Portable Electronic Devices. *InfoMat* 2019, *1*(1), 6–32. DOI: 10.1002/inf2.12000.

[4] Crabtree, G.; Kócs, E.; Trahey, L. The Energy-Storage Frontier: Lithium-Ion Batteries and Beyond. *MRS Bull.* 2015, *40*(12), 1067–1078. DOI: 10.1557/mrs.2015.259.

[5] Zubi, G.; Dufo-López, R.; Carvalho, M.; Pasaoglu, G. The Lithium-Ion Battery: State of the Art and Future Perspectives. *Renewable Sustain. Energy Rev.* 2018, *89*, 292–308. DOI: 10.1016/j.rser.2018.03.002.

[6] Soares, V. O.; Rodrigues, A. M. Improvements on Sintering and Thermal Expansion of Lithium Aluminum Silicate Glass-Ceramics. *Ceram. Int.* 2020, *46*(11), 17430–17436. DOI: 10.1016/j.ceramint.2020.04.037.

[7] Alves, M. F. R. P.; Simba, B. G.; Fernandes, M. H. F. V.; Elias, C. N.; Amarante, J. E. V.; dos Santos, C. Effect of Heat Treatment on the Roughness and Mechanical Properties of Dental Lithium Disilicate Glass-Ceramics. *Ceram. Int.* 2022, *48*(18), 26303–26311. DOI: 10.1016/j.ceramint.2022.05.314.

[8] Krause, F. C.; Ruiz, J.-P.; Jones, S. C.; Brandon, E. J.; Darcy, E. C.; Iannello, C. J.; Bugga, R. V. Performance of Commercial Li-Ion Cells for Future NASA Missions and Aerospace Applications. *J. Electrochem. Soc.* 2021, *168*(4), 040504. DOI: 10.1149/1945-7111/abf05f.

[9] Marmol, F. Lithium: Bipolar Disorder and Neurodegenerative Diseases Possible Cellular Mechanisms of the Therapeutic Effects of Lithium. *Prog. Neuropsychopharmacol. Biol. Psychiatry* 2008, *32*(8), 1761–1771. DOI: 10.1016/j.pnpbp.2008.08.012.

[10] Kavanagh, L.; Keohane, J.; Garcia Cabellos, G.; Lloyd, A.; Cleary, J. Global Lithium Sources—Industrial Use and Future in the Electric Vehicle Industry: A Review. *Resources* 2018, *7*(3), 57. DOI: 10.3390/resources7030057.

[11] Calvo, G.; Valero, A. Strategic Mineral Resources: Availability and Future Estimations for the Renewable Energy Sector. *Environ. Dev.* 2022, *41*, 100640. DOI: 10.1016/j.envdev.2021.100640.

[12] Garcia, L. V.; Ho, Y.-C.; Myo Thant, M. M.; Han, D. S.; Lim, J. W. Lithium in a Sustainable Circular Economy: A Comprehensive Review. *Processes* 2023, *11*(2), 418. DOI: 10.3390/pr11020418.

[13] Sanjuan, B.; Gourcerol, B.; Millot, R.; Rettenmaier, D.; Jeandel, E.; Rombaut, A. Lithium-Rich Geothermal Brines in Europe: An Up-Date About Geochemical Characteristics and

Implications for Potential Li Resources. *Geothermics* 2022, *101*, 102385. DOI: 10.1016/j. geothermics.2022.102385.

[14] Chandrasekharam, D.; Şener, M. F.; Recepoğlu, Y. K.; Isık, T.; Demir, M. M.; Baba, A. Lithium: An Energy Transition Element, Its Role in the Future Energy Demand and Carbon Emissions Mitigation Strategy. *Geothermics* 2024, *119*, 102959. DOI: 10.1016/j. geothermics.2024.102959.

[15] Ni, C.; Liu, C.; Wang, J.; Liang, Y.; Xie, W.; Zhong, H.; He, Z. Advances and Promotion Strategies of Processes for Extracting Lithium from Mineral Resources. *J. Ind. Eng. Chem.* 2024. DOI: 10.1016/j.jiec.2024.05.052.

[16] Li, H.; Eksteen, J.; Kuang, G. Recovery of Lithium from Mineral Resources: State-Of-The -Art and Perspectives–A Review. *Hydrometallurgy* 2019, *189*, 105129. DOI: 10.1016/j. hydromet.2019.105129.

[17] Karrech, A.; Azadi, M. R.; Elchalakani, M.; Shahin, M. A.; Seibi, A. C. A Review on Methods for Liberating Lithium from Pegmatites. *Miner. Eng.* 2020, *145*, 106085. DOI: 10.1016/j.mineng.2019.106085.

[18] Tadesse, B.; Makuei, F.; Albijanic, B.; Dyer, L. The Beneficiation of Lithium Minerals from Hard Rock Ores: A Review. *Miner. Eng.* 2019, *131*, 170–184. DOI: 10.1016/j. mineng.2018.11.023.

[19] Yoshizuka, K.; Nishihama, S.; Takano, M.; Asano, S. Lithium Recovery from Brines with Novel λ-MnO2 Adsorbent Synthesized by Hydrometallurgical Method. *Solvent Extr. Ion Exch.* 2021, *39*(5–6), 604–621. DOI: 10.1080/07366299.2021.1876443.

[20] Battaglia, G.; Berkemeyer, L.; Cipollina, A.; Cortina, J. L.; Fernandez de Labastida, M.; Lopez Rodriguez, J.; Winter, D. Recovery of Lithium Carbonate from Dilute Li-Rich Brine via Homogenous and Heterogeneous Precipitation. *Ind. Eng. Chem. Res.* 2022, *61* (36), 13589–13602. DOI: 10.1021/acs.iecr.2c01397.

[21] Yoshizuka, K.; Kitajou, A.; Holba, M. Selective Recovery of Lithium from Seawater Using a Novel MnO2 Type Adsorbent III-Benchmark Evaluation. *Ars. Separatoria Acta* 2006, *4*, 78–85.

[22] Recepoğlu, Y. K.; Kabay, N.; Yılmaz-Ipek, İ.; Arda, M.; Yoshizuka, K.; Nishihama, S.; Yüksel, M. Equilibrium and Kinetic Studies on Lithium Adsorption from Geothermal Water by λ-MnO2. *Solvent Extr. Ion Exch.* 2017, *35*(3), 221–231. DOI: 10.1080/ 07366299.2017.1319235.

[23] Recepoğlu, Y. K.; Kabay, N.; Yoshizuka, K.; Nishihama, S.; Yılmaz-Ipek, İ.; Arda, M.; Yüksel, M. Effect of Operational Conditions on Separation of Lithium from Geothermal Water by λ-MnO2 Using Ion Exchange–Membrane Filtration Hybrid Process. *Solvent Extr. Ion Exch.* 2018, *36*(5), 499–512. DOI: 10.1080/07366299.2018.1529232.

[24] Onishi, K.; Nakamura, T.; Nishihama, S.; Yoshizuka, K. Synergistic Solvent Impregnated Resin for Adsorptive Separation of Lithium Ion. *Ind. Eng. Chem. Res.* 2010, *49*(14), 6554–6558. DOI: 10.1021/ie100145d.

[25] Guo, F.; Nishihama, S.; Yoshizuka, K. Selective Recovery of Valuable Metals from Spent Li-Ion Batteries Using Solvent-Impregnated Resins. *Environ. Technol.* 2013, *34*(10), 1307–1317. DOI: 10.1080/09593330.2012.746734.

[26] Arroyo, F.; Morillo, J.; Usero, J.; Rosado, D.; El Bakouri, H. Lithium Recovery from Desalination Brines Using Specific Ion-Exchange Resins. *Desalination.* 2019, *468*, 114073. DOI: 10.1016/j.desal.2019.114073.

[27] Çiçek, A.; Yilmaz, O.; Arar, Ö. Removal of Lithium from Water by Aminomethylphosphonic Acid-Containing Resin. *J. Serb. Chem. Soc.* 2018, *83*(9), 1059–1069. DOI: 10.2298/JSC170930020C.

[28] Recepoğlu, Y. K.; Kabay, N.; Ipek, I. Y.; Arda, M.; Yüksel, M.; Yoshizuka, K.; Nishihama, S. Packed Bed Column Dynamic Study for Boron Removal from

Geothermal Brine by a Chelating Fiber and Breakthrough Curve Analysis by Using Mathematical Models. *Desalination*. 2018, *437*(February), 1–6. DOI: 10.1016/j.desal.2018.02.022.

[29] Recepoğlu, Y. K.; Kabay, N.; Yılmaz-İpek, İ.; Arda, M.; Yüksel, M.; Yoshizuka, K.; Nishihama, S. Deboronation of Geothermal Water Using N-Methyl-D-Glucamine Based Chelating Resins and a Novel Fiber Adsorbent: Batch and Column Studies. *J. Chem. Technol. Biotechnol.* 2017, *92*(7), 1540–1547. DOI: 10.1002/jctb.5234.

[30] Yilmaz-Ipek, I.; Koseoglu, P.; Yuksel, U.; Yasar, N.; Yolseven, G.; Yuksel, M.; Kabay, N. Separation of Boron from Geothermal Water Using a Boron Selective Macroporous Weak Base Anion Exchange Resin. *Sep. Sci. Technol.* 2010, *45*(6), 809–813. DOI: 10.1080/01496391003607357.

[31] Langmuir, I. The Constitution and Fundamental Properties of Solids and Liquids. Part I. Solids. *J. Am. Chem. Soc.* 1916, *38*(11), 2221–2295. DOI: 10.1021/ja02268a002.

[32] Freundlich, H. Über Die Adsorption in Lösungen. *Z. für physikalische Chem.* 1907, *57*(1), 385–470. DOI: 10.1515/zpch-1907-5723.

[33] Nguyen, C.; Do, D. D. The Dubinin–Radushkevich Equation and the Underlying Microscopic Adsorption Description. *Carbon N Y* 2001, *39*(9), 1327–1336. DOI: 10.1016/S0008-6223(00)00265-7.

[34] Babkin, A.; Burakova, I.; Burakov, A.; Kurnosov, D.; Galunin, E.; Tkachev, A.; Ali, I. Adsorption of Cu2+, Zn2+ and Pb2+ Ions on a Novel Graphene-Containing Nanocomposite: An Isotherm Study. In *IOP Conference Series: Materials Science and Engineering*. IOP Publishing: Tambov, Russia, 2019; Vol. 693, pp 012045.

[35] Recepoğlu, Y. K.; Arabacı, B.; Kahvecioğlu, A.; Yüksel, A. Granulation of Hydrometallurgically Synthesized Spinel Lithium Manganese Oxide Using Cross-Linked Chitosan for Lithium Adsorption from Water. *J. Chromatogr. A* 2024, *1719*, 464712. DOI: 10.1016/j.chroma.2024.464712.

[36] Weber, W. J.; Morris, J. C. Kinetics of Adsorption on Carbon from Solution. *J. Sanit. Engrg. Div.* 1963, *89*(2), 31–59. DOI: 10.1061/JSEDAI.0000430.

[37] Jiang, H.; Yang, Y.; Yu, J. Application of Concentration-Dependent HSDM to the Lithium Adsorption from Brine in Fixed Bed Columns. *Sep. Purif. Technol.* 2020, *241*, 116682. DOI: 10.1016/j.seppur.2020.116682.

[38] Recepoğlu, Y. K.; Yüksel, A. Cross-Linked Phosphorylated Cellulose as a Potential Sorbent for Lithium Extraction from Water: Dynamic Column Studies and Modeling. *ACS Omega* 2022, *7*(43), 38957–38968. DOI: 10.1021/acsomega.2c04712.

[39] Taka, A. L.; Klink, M. J.; Mbianda, X. Y.; Naidoo, E. B. Chitosan Nanocomposites for Water Treatment by Fixed-Bed Continuous Flow Column Adsorption: A Review. *Carbohydr. Polym.* 2021, *255*, 117398. DOI: 10.1016/j.carbpol.2020.117398.

[40] Aljarrah, S.; Alsabbagh, A.; Almahasneh, M. Selective Recovery of Lithium from Dead Sea End Brines Using UBK10 Ion Exchange Resin. *Can. J. Chem. Eng.* 2023, *101*(3), 1185–1194. DOI: 10.1002/cjce.24559.

[41] Fukuda, H. Lithium Extraction from Brine with Ion Exchange Resin and Ferric Phosphate. Master Thesis, The University of British Columbia, Vancouver, 2019.

[42] Ventura, S.; Bhamidi, S.; Hornbostel, M.; Nagar, A.; Perea, E. *Selective Recovery of Metals from Geothermal Brines*; SRI International: Menlo Park, CA, 2016.

[43] Luo, X.; Guo, B.; Luo, J.; Deng, F.; Zhang, S.; Luo, S.; Crittenden, J. Recovery of Lithium from Wastewater Using Development of Li Ion-Imprinted Polymers. *ACS Sustain. Chem. Eng.* 2015, *3*(3), 460–467. DOI: 10.1021/sc500659h.